CFD validation of optimized compact heat exchanger designs

Johan R. Espelund, Geir Skaugen

SINTEF Energy Research, Sem Sælands vei 11, Trondheim, Norway
Corresponding author: geir.skaugen@sintef.no

Abstract: In offshore oil and gas production gas turbines are used for both power production and to provide process heat. CO_2 emissions from the gas turbines accounts for about 25 % of the total Norwegian emissions and installing a bottoming cycle to produce power by recovering heat from the gas turbine exhaust is one way to reduce these missions. When installing a steam bottoming cycle offshore, the total weight and size will be important, and there is a need for a compact heat recovery steam generator (HRSG). A compact HRSG will often need to be designed with smaller tube diameters than conventional on-shore steam generators. To increase confidence in the compact design, the heat transfer and pressure loss models need to be accurate for the relevant geometry ranges. In this work, a compact Once Through Steam Generator (OTSG) is designed using optimisation procedures where the total weight of the steam generator has been minimised for a desired duty with restrictions for pressure losses. A range of correlations from the literature were used for the calculation of the performance. The results from the optimisation show that the 'heaviest' results were about three times the minimum weight than the 'lightest'. To increase confidence in the results, and to provide a recommendation for design models, a validated CFD model was used to perform a numerical analysis of the optimised geometry and compare this with the correlations.

Keywords: heat exchanger optimization, finned tube bundle, heat transfer, pressure drop, CFD

1. INTRODUCTION

The oil and gas industry is a significant contributor to the Norwegian overall emissions, with offshore installations accounting for a quarter of total greenhouse gas emissions. Most of these emissions come from gas turbines used on the platforms. To reduce CO_2 emissions towards 2030, the installation of steam bottoming cycles for power production has been proposed as illustrated in Fig. 1. Another technology to reduce emissions from gas turbines is to use carbon-free fuels like for instance mixtures including ammonia and hydrogen. Then the fuels must be imported off-shore and installing a bottoming cycle will have considerable fuel-saving potential. Weight and size of these cycles are

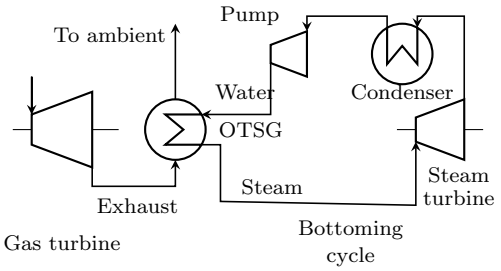

Fig. 1. Gas turbine with a steam bottoming cycle.

currently limiting factors for their widespread implementation, and efforts have already been made to develop designs that meet these criteria. Previous studies have shown that using small diameter tubes in the heat exchanger is one of the key factors in achieving compact design. However, the design of the heat exchanger currently relies on empirical correlations that are not necessarily validated for offshore geometries. As a result, designs can vary greatly depending on which correlation is chosen. Mazzetti et al. (2021) and Deng et al. (2021) developed an optimisation procedure for steam bottoming cycle design, which demonstrated that the heat recovery steam generator (HRSG) was the main contributor to the total weight of the cycle. They showed that optimising the HRSG with minimum weight as the objective, the lowest possible tube diameter was always selected In Montañés et al. (2023), a similar optimisation study for a combined heat and power bottoming steam cycle was done. Here, typical available tube diameters and wall thicknesses were chosen for the HRSG while the remaining geometry parameters were optimized. The results showed a clear trend on how the obtained minimum weight increased with the selected tube diameter. The fin height and the fin- and tube spacing were different for each tube diameter. To increase the confidence in these results and alternative to experimental work, numerical studies with CFD can be an option. Lindqvist and Næss Lindqvist and Næss (2018) developed a steady-state CFD model for plain and serrated fin tube bundles, which was validated against available experimental data. The layout angle was limited to 30°, and both solid and serrated fins were investigated. A periodic domain was used, where a single tube row is modeled. The results were compared to a simulation where 8 tube rows were modeled, and it was found that the periodic model provided near identical results at a fraction of the computational cost. The numerical results were also compared with some widely used correlations,

[1] This publication has been funded by HighEFF - Centre for an Energy Efficient and Competitive Industry for the Future, an 8-year Research Centre under the FME-scheme (Centre for Environment-friendly Energy Research, 257632/E20). The authors gratefully acknowledge the financial support from the Research Council of Norway and user partners of HighEFF.

showing that the CFD model generally was more accurate than the correlations, being within 20 % of experimental values. It was found that none of the investigated empirical correlations yielded results similar to those of the CFD model for all geometries.

The current author, Espelund et al. (2022), expanded on this work by including tube bundles also with larger layout angles. It was found that the steady-state approach did not converge for larger angles, but transient simulations gave accurate results. Comparisons with experiments showed that the transient CFD model agreed within 20 %.

In this work, an optimised set of design parameters using the different exhaust side heat transfer and pressure loss models from Table 1 are found and the different minimum weights are compared. In earlier studies of compact Once Through Steam Generators (OTSG's) by Mazzetti et al. (2021), Deng et al. (2021), and Montañés et al. (2023), the ESCOA correlations have been used as the basis for the thermal design. Therefore, the thermal performance (duty and exhaust side pressure loss) when using the other models with the optimized "ESCOA geometry" has been evaluated as a pure simulation. Simulated Nu- and Eu-number are compared to the results from the CFD analysis.

2. GEOMETRIES AND CORRELATIONS

The heat recovery heat exchanger in a steam bottoming cycle can be a Once Through Steam Generator (OTSG). The OTSG geometry consists of finned tube bundles, either as a single core or divided into different bundles, each representing the economizer, the evaporator, and the superheater. In this case study, a single tube bundle is used as the base case. Relevant OTSG geometry parameters are illustrated in Fig. 2. A staggered tube pattern is used with a fixed layout angle of 30° as shown in Fig. 2(a). In this study, only models for solid round fins have been evaluated. Figure 2(c) shows the notation for the number of passes and rows per pass. The number of tubes per row N_t, is the number of tubes along a header.

The performance of the OTSG is calculated as a cross-counter flow heat exchanger with exhaust flowing upward. The exhaust flow is flowing across 60 tube rows $(30 \cdot 2)$. Each parallel circuit, "tubes per row", is defined to have equal performance so the problem is 2-dimensional. Each tube pass is divided into 20 sub-elements and the heat balance between gas and water/steam is solved for each of the the 1200 heat exchanger elements. For each sub-element the transferred heat, Q, is calculated from

$$Q = U \cdot A \cdot \Delta T. \tag{1}$$

The overall heat transfer coefficient U $(\mathrm{W/(m^2\,K)})$ is calculated from (2) based on internal and external heat transfer coefficient, α_i and α_o, the tube side and fin side surface areas, A_i and A_o, and the conductive resistance through the tube wall, R_w.

$$U = \left[\frac{1}{\alpha} \cdot \frac{A_o}{A_i} + R_w + \frac{1}{\alpha_o} \right] \tag{2}$$

In the performance calculations, the correlation from Bennett and Chen (1980) is used for the two-phase heat transfer when evaluating α_i in (2). Two-phase frictional pressure loss is calculated with the Friedel (1979) correlation. The extended surface "apparent" heat transfer coefficient α_o in Eq. (2) is calculated from a correlation for the Colburn j-factor or Nu-number that uses the detailed fin and tube geometry into account. The derived heat transfer coefficient is the α_c in Eq. (3) where η_f is the fin efficiency, A_f is the fin surface area and A_o is the total outside surface area.

$$\alpha_o = \alpha_c \cdot \left[1 - (1 - \eta_f) \frac{A_f}{A_o} \right] \tag{3}$$

The relations between the heat transfer coefficient α_c, the j-factor, Stanton- (St), Prandl- (PR) and the Nusselt (Nu) -number are shown in Eqs. (4) and (6).

$$j = \mathrm{St}\ \mathrm{Pr}^{2/3} = \alpha_c \frac{\mathrm{Pr}^{2/3}}{\rho \cdot u_{\max} \cdot c_p} \tag{4}$$

$$\mathrm{Nu} = \frac{\alpha_c d_h}{\lambda} \tag{5}$$

$$\mathrm{Pr} = \frac{\eta \cdot C_p}{\lambda} \tag{6}$$

where η (Pa s) is the dynamic viscosity, C_p (J/(kg K))is the specific heat capacity, λ (W/(m K)) is the thermal conductivity and d_h is the hydraulic diameter. The Re-number is based on the maximum velocity, $u_{\max}$ inside the tube bundle and with the hydraulic diameter as the diameter at the fin base, namely

$$\mathrm{Re} = \frac{u_{\max} d_h}{\nu}. \tag{7}$$

We have assumed L-fin where the fin base diameter, so the hydraulic diameter, d_h, is the outside tube diameter d_o plus $2 \cdot F_t$ where F_t is the fin thickness. The fin efficiency η_f in Eq. (3) is calculated as recommended by the correlation while the temperature difference ΔT in Eq. (1) is calculated for the arithmetic mean temperature difference between inlet and outlet fluid temperatures on inside and outside. Since the performance calculation model is called from an optimisation routine, we want to avoid unnecessary iterations so the OTSG is solved from the "warm" end, following the exhaust flow from the warm inlet. From a desired steam outlet temperature and pressure, the calculation is done backward to the feed water flow direction inside the tubes. When solved, the unknown inlet state for the steam and outlet state for the exhaust can be found. To solve the heat balance in each integration step, the 2'nd order Heun's method is used to accurately predict the temperature difference and the transferred heat, Q, from the warm to the cold end. After the integration, the total heat duty and the pressure losses for the exhaust and waterside are known and used by the optimisation routine in the constraint evaluations. The various correlations used for heat transfer and pressure loss on the exhaust side are listed along with the in Table 1

The pressure drop is calculated using the Euler number Eu, which is defined as the pressure drop across a tube row normalized by the dynamic pressure,

$$\mathrm{Eu} = \frac{\Delta p}{\frac{1}{2}\rho u_{F_{min}}^2} \tag{8}$$

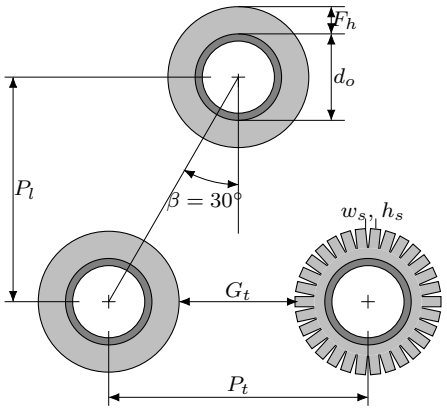

(a) Staggered tube pattern showing solid and serrated fins

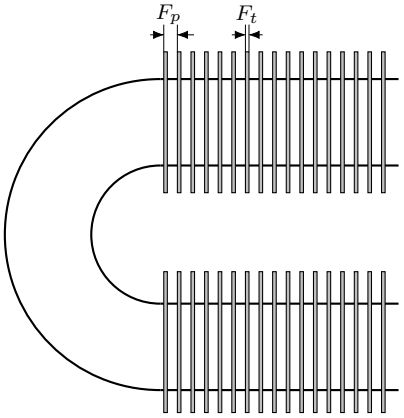

(b) Tubes with circular fins

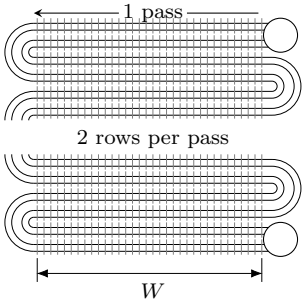

(c) Number of passes and rows per pass

Parameter	Unit	Value
Fin height, F_h	mm	4.0 - 25
Fin pitch, F_p	mm	2.0 - 8.0
Fin thickness, F_t	mm	1.05
Tube outer diameter, d_o	mm	25.4
Wall thickness	mm	2.11
Transversal/diagonal fin gap, G_t	mm	1.5 - 100
Core width, W	m	3.0 - 10.0
Number of passes, N_p	-	30
Rows per pass, N_r	-	2
Tubes per row, N_t	-	30 - 80
Layout angle, β	°	30
Transversal tube pitch, P_t	mm	Calculated
Longitudinal tube pitch, P_l	mm	Calculated

(d) Fixed and variable design parameters for the OTSG

Fig. 2. Geometry definitions for the OTSG used by the design optimisation model.

where Δp is the pressure drop across one tube row and $U_{F_{min}}$ is the velocity through the minimum flow area.

Table 1. List of evaluated correlations for outside heat transfer and pressure loss for round solid fins

Correlation	Heat transfer Pressure loss
	Briggs and Young (1963)
Briggs & Robinson	Robinson and Briggs (1966)
Stasiulevicius	Stasiulevicius et al. (1988)
PFR	Rosenman (1976)
Mon	Mon (2003)
ESDU	Hewitt (1998) (ch 2.5.3)
ESCOA	See. Ganapathy (2003)
Holfeld	Holfeld (2016)
Lindqvist	Lindqvist (2019)
Rabas	Rabas et al. (1981)

3. OPTIMIZATION PROCEDURE

The optimisation procedure is set up as a flowsheet optimisation model with only the OTSG as a single unit model. It is implemented in an in-house heat exchanger modelling software by Skaugen et al. (2013). The optimisation was done with the NLPQL model from Schittkowski (1986). NLPQL requires a function for the calculation of an objective and functions for the calculation of all equality and inequality constraints.

The optimisation model in this work is configured to minimise the weight of the OTSG in Fig. 1 for a given steam production and duty. The steam turbine and other components in the steam cycle are not included. The gas turbine is a natural gas-fired gas turbine with around 30 MW power output. The exhaust flow rate is 86.1 kg/s with a temperature of 510°. The corresponding water/steam boundary conditions used are: Feed water flow rate and temperature of 10.2 kg/s and 17.0 °C. The inlet feed water pressure is 29.5 bar.

The geometry design parameters, and their range, are listed in Table 2d. These are the free optimisation variables for the problem.

The underlying heat exchanger model consists of the *thermal simulation model* described in Sec. 2 combined with *weight calculation model* for the fin and tube weights plus an estimation for the total weight of the casing with plates, beams, and insulation. So, for a set of geometry input parameters, the free optimisation variables, the thermal model finds the transferred heat and pressure losses while the weight model estimates the total weight. The calculated results are converted into constraints and objective for the optimisation routine. By minimising the total weight, and not only the bundle weight, the model ensures that the size and shape of the tube bundle will require unnecessary large inlet/exit transition ducts for instance. The tube bundle will typically account for about 50% or less of the total weight for the OTSG. The optimisation problem is defined in Table 2. The condition for the required duty is the only equality constraint. NLQPL evaluates the constraints and the objective function and

proposes a new set of design variables (from Table until the minimum is found and none of the constraints are violated.

Table 2. Defined constraints and objective function for the optimisation problem

Description	Condition	
OTSG Duty	$Q = 34$	
Exhaust pressure loss	Δp_{ex}	
Water/steam pressure loss	Δp_{ws}	
Maximum exhaust velocity	$U_{\max}$	/s
Diagonal tube pitch	$P_d < 3$	
Objective	min (Total weight)	

The optimisation routine does not guarantee that the global minimum is found, so to improve confidence in the result a multi-start where each case has been run with 10 random sets of initial values for the free variables within the specified range.

4. CFD MODEL

A CFD model for plain and serrated fin tube banks has previously been developed by the current author (Espelund et al., 2022). A detailed description can be found in (Espelund,2022), but a summary of the model is given here. The simulations were run on the IDUN HPC cluster (Själander et al. 2021). The incompressible Navier-Stokes equations are solved for the external flue gas in a periodic domain, while the heat equation is solved in the fins. The domains are coupled with thermal boundary conditions, and the equations are solved using the `chtMultiRegionFoam` solver in OpenFOAM v2206.

4.1 Governing equations

The Navier-Stokes equations are solved in the gas region. They are constituted by the continuity, momentum, and energy equations. In this section, Einstein notation is used, with $i \in \{1, 2, 3\}$ corresponding to the three spatial coordinates. The continuity equation reads,

$$\frac{\partial u_i}{\partial x_i} = 0, \tag{9}$$

where u_i is the velocity component in the i direction. The gas is modelled as incompressible and with constant thermal and transport properties, yielding the following momentum balance equations,

$$\frac{\partial u_i}{\partial x_j} = -\frac{1}{\rho}\frac{\partial p}{\partial x_i} + \nu_{\text{eff}}\frac{\partial^2 u_i}{\partial x_j x_j} + S_i, \tag{10}$$

where p is the pressure field, ρ is the density and ν_{eff} is the effective kinematic viscosity (accounting for both molecular and turbulent viscosity). The turbulence model by Spalart and Allmaras (1992) is used. S_i is an external driving force (corresponds to the pressure loss $\frac{\partial p}{\partial x_i}$) to drive the flow through the cyclic domain, as described by Patankar et al. (1977).

The energy conservation equation is formulated using the specific enthalpy h, viz.

$$\frac{\partial(\rho h + e_{\text{K}})}{\partial t} + \frac{\partial}{\partial x_i}\left(u_i(\rho h + e_{\text{K}})\right) - \frac{\text{D}p}{\text{D}t} = -\frac{\partial q_i}{\partial x_i}, \tag{11}$$

where the heat flux is given by Fourier's law $q_i = \rho\alpha_{\text{eff}}\,\partial h/\partial x_i$, where the effective thermal diffusivity is defined as $\alpha_{\text{eff}} = \kappa_{\text{eff}}/(\rho c_{\text{p}})$ and $e_{\text{K}} = \frac{1}{2}\rho u_i u_i$ is the specific kinetic energy. Here κ_{eff} is the effective thermal conductivity. In the solid region, the special case of $u_i = \text{D}p/\text{D}t = 0$ in Equation (11) is solved. The solid region is also assumed to have constant thermal properties.

To reduce the time needed to reach pseudo-steady-state conditions, steady-state simulations are run initially, using the *chtMultiRegionSimpleFoam* solver. Once the average fin temperature T_f stabilises, the steady-state simulation is terminated, and the transient simulation is initiated. To ensure converged results and a sufficiently long sampling interval, the transient simulations were run for 30 fluid exchange times $\tau = P_l/U_{F,max}$. Data were sampled for $\tau > 15$.

4.2 Geometry and discretization

A periodic domain is used to model the heat exchanger, and the discretization follows the procedure in Lindqvist and Næss (2018). The geometry is specified according to the optimised solid fin OTSG. The mesh consists of hexahedral cells, with wall refinement at the fins sides and at the tube surface. The mesh at the edges of the fins are not refined towards the wall boundary, which means that wall functions are needed to model the turbulent profiles here. The numerical mesh is illustrated in Fig. 4.

4.3 Boundary conditions

By adding an external pressure force S_i in the momentum equation, Eq. (10), cyclic boundary conditions can be used in all directions. As the pressure gradient is not known a priori, the *meanVelocityForce* option is used in OpenFOAM. This will adjust the source term to reach a specified mean velocity, which was used to fix Re to relevant values from the optimized OTSG design.

The temperature field needs additional treatment since the total heat transfer to the domain is not known a priori. To keep a fixed average inlet temperature, a *cyclic jump* boundary condition is used between the inlet and outlet for temperature.

$$T_{\text{in}}(x,y) = T_{\text{w}} + \frac{T_{\text{out}}(x,y) - T_w}{\overline{T_{\text{out}}} - \underset{w}{T}} \cdot (T_{\text{in,target}} - T_w), \tag{12}$$

where $T_{\text{in}}(x,y)$ and $T_{\text{out}}(x,y)$ is the inlet and outlet temperature fields, respectively, T_{w} is the constant wall temperature and $T_{\text{in,target}}$ is the constant target inlet temperature. The average temperature is defined as

$$\overline{T} = \frac{1}{\dot{m}}\int_A T(x,y)\rho u_i dn_i, \quad \text{where} \quad \dot{m} = \int_A \rho u_i dn_i, \tag{13}$$

and n_i is the patch normal vector and A is the domain of the patch. Thus, this is a mass flux weighted average which ensures a fixed inlet temperature, but with a cyclic profile that also ensures that the temperature is constant at the walls. In this work, the conditions of $T_{\text{in}} = 320\,\text{K}$ and $T_{\text{w}} = 300\,\text{K}$ has been used, which corresponds to experimental conditions for correlation development.

At the interface between the gas and solid regions, no-slip and no-penetration are prescribed the velocity field and

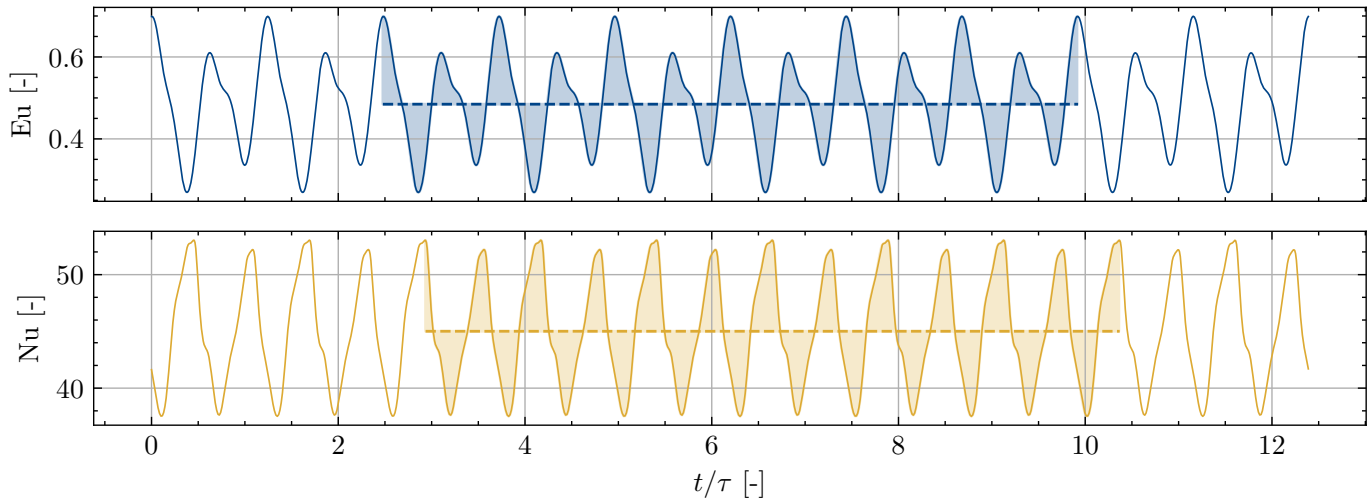

Fig. 3. Illustration of sampling. Time signal for Eu and Nu, with the sampling region shaded around the time average value. The signals are from the coarsest mesh simulation with Re = 7500 The illustration shows 6 periods used for sampling, while the actual sampling was performed with 15 periods.

von Neumann-boundary conditions for the pressure. The temperature field is coupled in the two domains and obeys continuity in temperature and energy conservation, i.e.

$$T_{\mathrm{w,gas}} = T_{\mathrm{w,fin}} \quad \text{and} \quad q_i n_i|_{\mathrm{w,gas}} = -q_i n_i|_{\mathrm{w,fin}}, \tag{14}$$

where n_i is the wall normal direction.

4.4 Post-processing

The transient temperature, heat flux and pressure drop data were time averaged as

$$X = \frac{1}{t_2 - t_1} \int_{t_1}^{t_2} x(t) dt, \tag{15}$$

where t_1 and t_2 is the start and end time of the sampling interval, respectively. $x(t)$ is the transient time signal and X is the time average. The sampling of Nu and Eu is illustrated in Fig. 3.

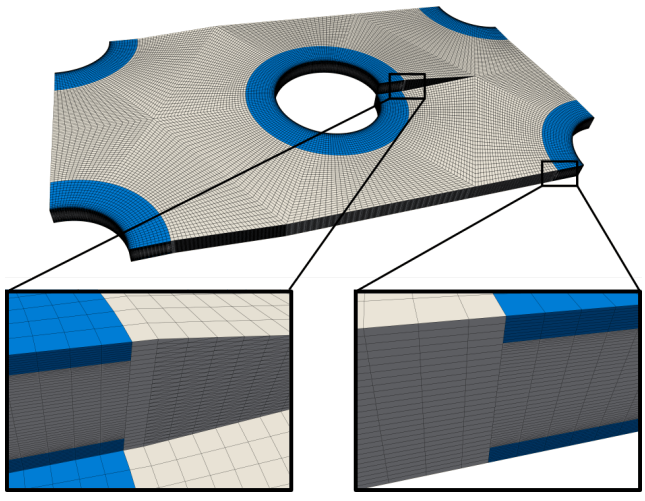

Fig. 4. Computational mesh used in the CFD simulations.

Eu is calculated directly by using Eq. (8), with $\Delta p = P_l \cdot \partial p/\partial x$. To calculate Nu, the temperature driving force ΔT in Eq. (1) needs to be extracted from the CFD simulations. This is taken to be the difference between the bulk gas temperature and the wall temperature

$$\Delta T = T_b - T_w, \tag{16}$$

where the bulk temperature is defined as

$$T_b = \overline{T_{\mathrm{front}}} + \overline{T_{\mathrm{back}}}, \tag{17}$$

where T_{front} and T_{back} are the temperature fields at the planes located at $-P_l/2$ and $+P_l/2$ relative to the center tube, respectively.

The heat flux and fin temperatures are sampled at the center tube, and Nu is then calculated using the definition in Eq. (5).

4.5 Thermophysical properties

The thermal and transport properties are assumed to be constant for both the gas and fins. They are summarised in Table 3. The fin region properties correspond to that of carbon SS-304 steel, while the gas phase is modelled as air at 310 K. These conditions correspond to the experimental conditions in which most correlations are developed.

Table 3. Constant thermophysical properties used in the CFD simulations.

Property	**Gas**	**Fins**
Density, ρ (kg/m^3)	1.1614	7950
Specific Heat Capacity, C_p (J/kg·K)	1007	520
Thermal Conductivity, κ (W/m·K)	0.0263	15.5
Dynamic Viscosity, (Pa·s)	1.8455×10^{-5}	–

4.6 Grid refinement study

To assess the grid sensitivity of the solution, a grid refinement study was performed. The simulations were run with

Re = 7 500 using four different mesh resolutions, where the wall cell sizes were equal for all meshes, ensuring the same y^+ values for each simulation. An initial steady-state simulation was conducted using the coarsest mesh, and its final time step was used as the initial condition for all simulations in the grid refinement study. The simulations were run until a quasi-steady state was achieved, where the time-averaged values of Eu and Nu did not change significantly. The resulting values are presented in Fig. 5. A mesh resolution of 730 000 cells was deemed sufficient, as both Eu and Nu are within 1 % of the values at the finest grid (1 850 000 cells).

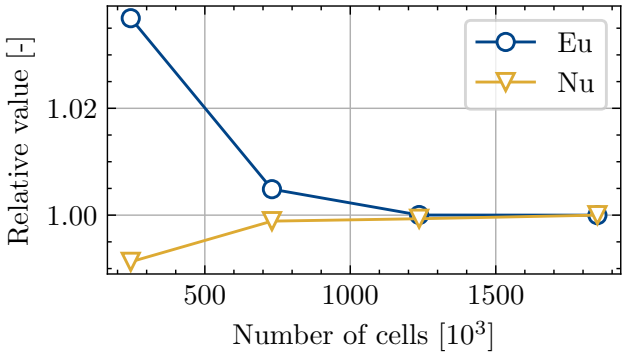

Fig. 5. Results from grid refinement study. Eu and Nu are normalised by the value at the finest grid.

5. RESULTS AND DISCUSSION

5.1 Results from optimisation

The main results from the optimisation are shown in Table 4 and are an indication of the different models ability to extrapolate. The optimisation is run twice. The first time the number of tubes per row is treated as a decimal number, providing a continuous flow area. As a second run, its value is a fixed integer value while the other three parameters, tube length, fin height, and fin pitch are re-optimised with a slight minimum weight increase as the penalty. It was also observed that all the models were constrained by the minimum tube pitch of 3 times the outer tube diameter, so a fixed triangular tube pitch of 76.2 mm was specified in the 2'nd optimisation run.

As seen from Table 4, the obtained minimum weights range from 84 to 124 tonnes. The tendency is that the models obtaining the lowest weight seem to favour very low fin- height (3-7.5 mm) and pitch below 4 mm while the others are generally in the range of 7-15 mm and 4-8 mm. In a practical situation, the fin height and pitch cannot be varied freely meaning that the spread in the weight could be larger depending on the underlying model. In an OTSG, the heat transfer on the outside is limiting, so therefore fins are used to increase the surface area. However, when optimising for a specific duty and minimising the total weight, the weight contribution from the fins seems to be significant, and thus the optimisation routine finds the alternative solutions as discussed above.

The optimal tube lengths generally are between 5 and 6 m with the number of tubes per row around 50. These two parameters make up the exhaust cross-flow area and

Table 4. The result for the free geometry variables and the objective function for the different models

Model	Tube length [m]	Tubes per row [-]	Fin height [mm]	Fin pitch [mm]	Minimum Weight [Ton]
Briggs	6.29	56	10.1	5.6	124.7
Holfeld	5.91	50	10.5	4.4	114.6
Lindqvist	6.84	52	14.1	9.7	109.6
Rabas	5.71	50	14.5	8.1	102.6
PFR	5.32	42	3.5	1.9	99.3
ESCOA	5.83	48	7.6	4.0	97.7
Mon	5.47	51	3.0	1.5	97.3
ESDU	5.41	49	6.2	3.5	91.5
Stasiulevicius	4.87	50	6.5	3.7	84.1

determine the size of the enclosing casing which accounts for about half the total weight

Each of the correlations from Table 1 has also been used to simulate the performance of the optimised geometry from the ESCOA models. In Fig. 6 the comparison between the predictions is shown.

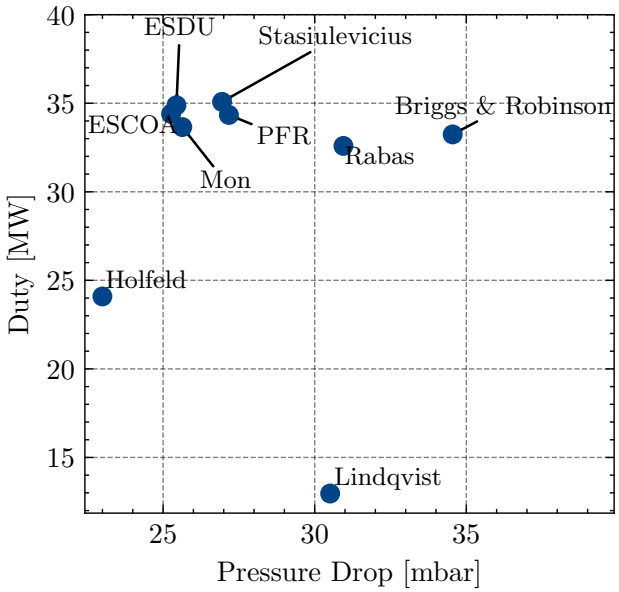

Fig. 6. Resulting duty and pressure losses for the simulation of the fixed geometry.

Some of the models predict the duty and pressure loss close to 34.4 MW and 25 mbar. Outliers seem to either predict the duty with too high pressure-loss. The correlation from Holfeld (2016) seems to underpredict both the duty and the pressure loss although this was developed based on experimental data that also included small-diameter tubes. A similar trend can be observed from Lindqvist and Næss (2018) that also were developed with compact geometries in mind.

5.2 Results from CFD simulations

Figure 7 presents the streamlines sampled during transient simulations at Re = 7500, coloured according to the normalised temperature. The figure also displays the temperature field of the fins. The streamlines distinctly illustrate vortex shedding occurring behind the tubes. This

vortex shedding is likely the primary cause of the significant oscillations observed in Eu and Nu, as depicted in Fig. 3. These oscillations were also observed after a certain number of iterations in the preliminary steady-state simulations, indicating that the steady-state assumption is un-physical. These oscillations are indicative of highly transient flow and heat transfer phenomena taking place within the OTSG, suggesting that steady-state simulations are not sufficient to model these flows accurately.

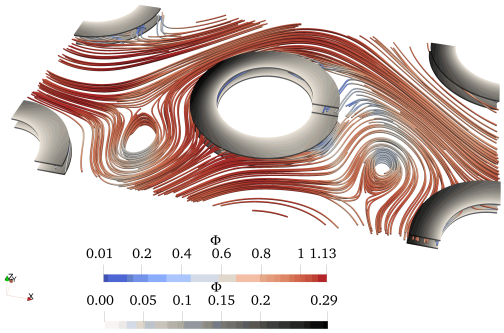

Fig. 7. Velocity streamlines and fins coloured by normalised temperature, for Re = 7 500. Here $\Phi = (T - T_w)/(T_{\text{in,target}} - T_w)$ is the normalised temperature.

Figure 8 shows that the correlation from Rabas et al. (1981) is closest to the CFD results for the Nu, with an average deviation of 6 %, while the model from Holfeld (2016) seem show best agreement for Eu, with an average deviation of 16 %. In general, most of the empirical correlations seem to overestimate the Eu and thus also predict a higher pressure loss, with the correlation by Lindqvist being the most extreme, deviating by 120 %. This correlation also has the largest deviation for Nu, with 53 %. In Fig. 6 the Holfeld-correlation shows the lowest pressure loss of all the models for the optimized geometry from using the ESCOA correlation. We note from looking at the streamlines in Fig. 7 that the geometry is quite "open" with regions with considerable turbulence and backflow. One might suspect that some local "pressure recovery" is not captured by any of the correlations. On the other hand, the correlation by Holfeld was designed with a bias toward compact geometries.

An additional optimisation, using the Stasiulevicius et al. (1988) correlation for the Nu and the Holfeld (2016) correlation for the Eu was performed.

The result from using these two models found a design with a very low fin pitch (1.07 mm) and with very low fins (2.2 mm). The resulting weight was 76.5 tons, about 20 tons less than the "reference" weight from the use of the ESCOA correlations. This design resembles a tube-bundle with low-fin tubes and this is probably not to be trusted to extrapolate a correlation developed for individually finned tubes to such type of low-fins. The more constrained the optimisation problem is, the more the minimum weight will increase. So, where weight is important, like in offshore installations, more experimental data or a systematic approach with CFD and machine learning would be useful to increase confidence in the design result.

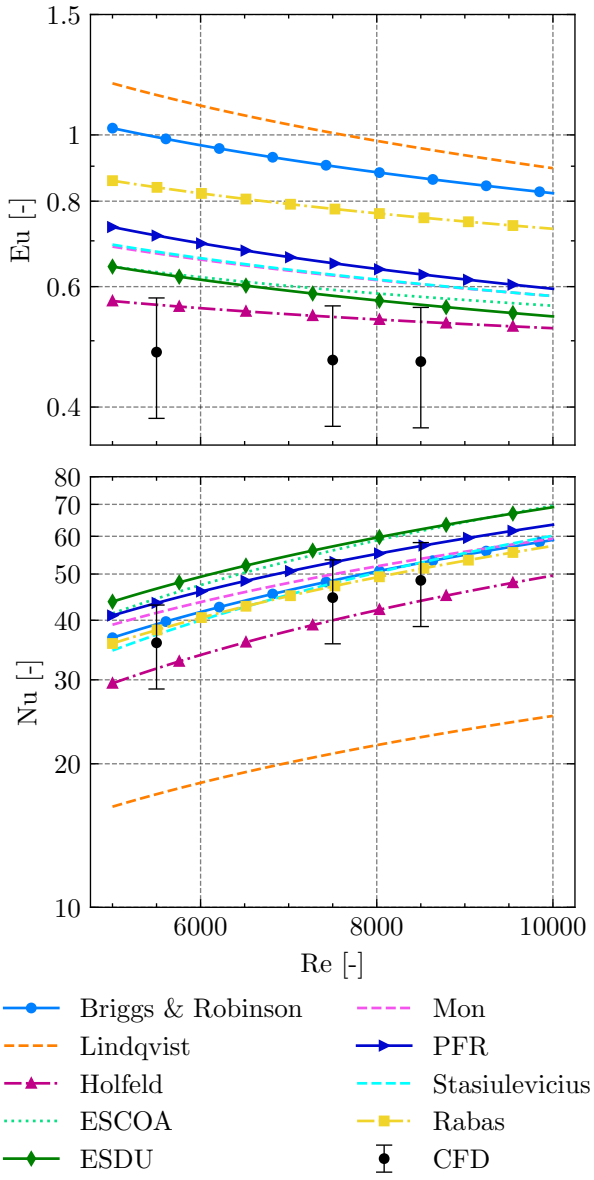

Fig. 8. Results from CFD simulations compared with empirical correlations. The bars on the CFD markers denote ±20 %.

6. CONCLUSIONS

In this work, we performed design optimisation of an offshore Once Through Steam Generator (OTSG) using nine different correlations to predict pressure loss and heat transfer. A reference optimised design was selected, and a validated CFD model was used to simulate pressure loss and heat transfer. The simulation results were compared against the correlations. The following conclusions were drawn:

- There is a significant variation in optimised designs, depending on the selected correlations.
- CFD results indicate transient behaviour in the selected configuration.
- A comparison with CFD data reveals significant deviations in pressure loss predictions for several correlations.

DOI: 10.3384/ecp212.010

- The "best" models appear to extrapolate excessively.
- Additional experimental data and/or a systematic CFD approach to developing new models would be beneficial.

Without a CFD analysis of the optimal geometries found for the typical outliers from Fig. 5, (Holfeld, Lindqvist, Rabas and Briggs and Young) for a cross-check, it is difficult to conclude and recommend which of the models that is suitable for designing a compact OTSG.

REFERENCES

Bennett, D.L. and Chen, J.C. (1980). Forced convective boiling in vertical tubes for saturated pure components and binary mixtures. *AIChE Journal*, 26(3), 454–461. doi:10.1002/aic.690260317. URL http://doi.wiley.com/10.1002/aic.690260317.

Briggs, D.E. and Young, E.H. (1963). Convection heat transfer and pressure drop of air flowing across triangular pitch banks of finned tubes. In *Chem. Eng. Prog. Symp. Ser*, volume 59, 1–10.

Deng, H., Skaugen, G., Næss, E., Zhang, M., and Øiseth, O.A. (2021). A novel methodology for design optimization of heat recovery steam generators with flow-induced vibration analysis. *Energy*, 226, 120325. doi:10.1016/j.energy.2021.120325.

Espelund, J.R., Meyer, O.H.H., and Skaugen, G. (2022). Numerical modelling of fin side heat transfer and pressure loss for compact heat recovery steam generators. 263–270. doi:10.3384/ecp192037. URL https://ecp.ep.liu.se/index.php/sims/article/view/521.

Espelund, J.R. (2022). Numerical modelling of fin side heat transfer and pressure loss for compact heat recovery steam generators. URL https://ntnuopen.ntnu.no/ntnu-xmlui/handle/11250/3016714. Accepted: 2022-09-08T17:19:43Z.

Friedel, L. (1979). Improved Friction Pressure Drop Correlations for Horizontal and Vertical Two-Phase Pipe Flow. In *European Two-Phase Flow Group Meeting*. Ispra, Italy.

Ganapathy, V. (2003). Heat Transfer Equipment Design and Performance. In *Industrial Boilers*, 9, 1689–1699. doi:10.1017/CBO9781107415324.004.

Hewitt, G. (1998). *Heat Exchanger Design Handbook, 1998*. Number pts. 1-2 in Heat Exchanger Design Handbook, 1998. Begell House.

Holfeld, A. (2016). *Experimental investigation of heat transfer and pressure drop in compact waste heat recovery units*. Doctoral thesis, NTNU.

Lindqvist, K. (2019). *Modeling of Flow and Heat Transfer in Karl Lindqvist Computational Fluid Dynamics Modeling of Flow and Heat Transfer in Fin-Tube Bundles*. Doctoral thesie, NTNU.

Lindqvist, K. and Næss, E. (2018). A validated CFD model of plain and serrated fin-tube bundles. *Applied Thermal Engineering*, 143, 72–79. doi:10.1016/j.applthermaleng.2018.07.060. URL https://www.sciencedirect.com/science/article/pii/S1359431117359598.

Mazzetti, M.J., Hagen, B.A.L., Skaugen, G., Lindqvist, K., Lundberg, S., and Kristensen, O.A. (2021). Achieving 50% weight reduction of offshore steam bottoming cycles. *Energy*, 230, 120634. doi:10.1016/j.energy.2021.120634. URL https://www.sciencedirect.com/science/article/pii/S0360544221008835.

Mon, M.S. (2003). Numerical investigation of air-side heat transfer and pressure drop in circular finned-tube heat exchangers. 151.

Montañés, R.M., Hagen, B., Deng, H., Skaugen, G., Morin, N., Andersen, M., and J. Mazzetti, M. (2023). Design optimization of compact gas turbine and steam combined cycles for combined heat and power production in a FPSO system–A case study. *Energy*, 282, 128401. doi:10.1016/j.energy.2023.128401.

Patankar, S.V., Liu, C.H., and Sparrow, E.M. (1977). Fully Developed Flow and Heat Transfer in Ducts Having Streamwise-Periodic Variations of Cross-Sectional Area. *Journal of Heat Transfer*, 99(2), 180–186. doi:10.1115/1.3450666. URL https://asmedigitalcollection.asme.org/heattransfer/article/99/2/180/382469/Fully-Developed-Flow-and-Heat-Transfer-in-Ducts.

Rabas, T., Eckels, P., and Sabatino, R. (1981). The effect of fin density on the heat transfer and pressure drop performance of low-finned tube banks. *Chemical Engineering Communications*, 10(1-3), 127–147. doi:10.1080/00986448108910930.

Robinson, K.K. and Briggs, D.E. (1966). Pressure drop of air flowing across triangular pitch banks of finned tubes. In *Chem. Eng. Prog. Symp. Ser*, volume 62, 177–184.

Rosenman, T. (1976). Heat transfer and pressure drop characteristics of dry tower extended surfaces. part i. heat transfer and pressure drop data. doi:10.2172/7334913. URL https://www.osti.gov/biblio/7334913.

Schittkowski, K. (1986). NLPQL: A fortran subroutine solving constrained nonlinear programming problems. *Annals of Operations Research*, 5(2), 485–500. doi:10.1007/BF02022087.

Själander, M., Jahre, M., Tufte, G., and Reissmann, N. (2021). EPIC: An Energy-Efficient, High-Performance GPGPU Computing Research Infrastructure. *arXiv:1912.05848 [cs]*. ArXiv: 1912.05848.

Skaugen, G., Kolsaker, K., Walnum, H.T., and Wilhelmsen, (2013). A flexible and robust modelling framework for multi-stream heat exchangers. 49, 95–104. doi:10.1016/j.compchemeng.2012.10.006. URL https://linkinghub.elsevier.com/retrieve/pii/S0098135412003067.

Spalart, P. and Allmaras, S. (1992). A one-equation turbulence model for aerodynamic flows. In *30th Aerospace Sciences Meeting and Exhibit*. American Institute of Aeronautics and Astronautics, Reno,NV,U.S.A. doi:10.2514/6.1992-439. URL https://arc.aiaa.org/doi/10.2514/6.1992-439.

Stasiulevicius, J., Skrinska, A., Zhukauskas, A., and Hewitt, G.F. (1988). *Heat transfer of finned tube bundles in crossflow*. Hemisphere Pub. Corp.